Macrocyclic [N_4^{2-}] Coordinated Nickel Complexes as Catalysts for the Formation of Oxalate by Electrochemical Reduction of Carbon Dioxide

Manfred Rudolph, Sylvana Dautz, and Ernst-Gottfried Jäger*

Contribution from the Institute of Inorganic Chemistry, Friedrich-Schiller-Universität, August-Bebel-Str. 2, 07743 Jena, Germany

Received April 10, 2000

Abstract: The macrocyclic nickel complexes shown in Figure 1 are able to catalyze the electrochemical reduction of CO_2 to oxalate. In the case of the complexes with R^2 = COOEt or COMe, the overall reaction can be interpreted in terms of an outer-sphere electron-transfer reaction (6) followed by a dimerization of the $CO_2^{\bullet-}$ radical anions (7), but the variation of the electron-transfer rate constants with the standard potentials points to a coordinative interaction between the complexes and the CO_2 molecule. Complexes without COOEt or COMe substitution in the R^2 position undergo a fast deactivation reaction (first order with respect to [CO_2]) that is even visible in the time scale of the cyclic voltammetric experiments. The results of the cyclic voltammetric investigations could be confirmed in preparative-scale electrolyses where the complex Ni−Etn(Me/COOEt)-Etn proved to be the most active and persistent redox catalyst for the electrochemical reduction of CO_2 to oxalate that has been described so far.

The electrochemical reduction of carbon dioxide catalyzed by metal complexes has attracted continuous attention over the past decades although only CO and(or) formate are usually produced in this way.[1−3] For this reason, there has been a growing interest in redox mediators that are able to catalyze the electrochemical reduction of CO_2 accompanied by carbon−carbon bond formation. The uncatalyzed electrochemical reduction on inert electrode materials such as mercury produces oxalate through a coupling reaction (2) of the $CO_2^{\bullet-}$ radical anions produced in the first step of the electrode reaction. However, the higher the CO_2 concentration, the more the CO production grows at the expense of oxalate. The reason for this behavior is the tendency of the nucleophilic $CO_2^{\bullet-}$ radical anion to react with Lewis acids to form adducts which are *more easily* reduced than the CO_2 molecule itself. In the simplest case, the carbon dioxide molecule can play the role of the Lewis acid (3) and the subsequent reduction of the $CO_2-CO_2^{\bullet-}$ adduct leads to carbon monoxide and carbonate (4).[4,5] The synergetic effect of Lewis acids as well as weak Brönstedt acids for the catalytic reduction of CO_2 to CO has also been described in the literature.[2,6,7]

Due to the very negative potential for a direct electrochemical reductive activation of CO_2 (−2.21 V vs SCE in aprotic solvents), the investigations on metal complex electrocatalysts have been focused mainly on the problem of facilitating the reduction of the carbon dioxide as much as possible. For thermodynamical reasons, the latter is only possible if the CO_2 reduction products are energetically stabilized by coordination on the metal center. In other words, the metal complex, ML, may serve as a Lewis acid and consequently the oxalate production may be disfavored by increasing the Lewis acidity of the metal complex. One strategy to overcome this problem has been found recently by using bi- and trinuclear metal complexes which are reduced in two subsequent single-electron steps.[8,9] This enables two $CO_2^{\bullet-}$ radical anions to be formed simultaneously, and the dimerization reaction of the $CO_2^{\bullet-}$ radical anions is predestined by the structure of the complex. Particularly noteworthy are the relatively positive potentials where these complexes catalyze the oxalate production, but a look at the cyclic voltammograms published in one of the papers[9] reveals that the rate constants for the catalytic regeneration of the redox mediators, albeit not reported by the authors, are rather small.

In principle, the dimerization of the $CO_2^{\bullet-}$ radical is a very fast reaction that needs not to be promoted by a special structure of the metal complex. Thus, other attempts to force a reductive dimerization of carbon dioxide by means of binuclear metal complex catalysts, such as Ni_2−Biscyclam, failed.[10] It seems to be more important that the complex does not offer other pathways for a further reduction of the $CO_2^{\bullet-}$ species. The latter requires (a) a metal complex redox catalyst with a high electron donator activity in the reduced form to produce a high concentration of $CO_2^{\bullet-}$ radical anions to favor the reactions

$$ML^- + CO_2 \rightarrow ML + CO_2^{\bullet-} \quad (1)$$

$$2CO_2^{\bullet-} \rightarrow C_2O_4^{2-} \quad (2)$$

(1) Hawecker, J.; Lehn, J.-M.; Ziessel, R. *J. Chem. Soc., Chem. Commun.* **1984**, 328.
(2) Bhugun, I.; Lexa, D.; Saveant, J.-M. *J. Am. Chem. Soc*. **1996**, *118*, 1769.
(3) Beley, M.; Collin, J.-P.; Ruppert, R.; Sauvage, J.-P. *J. Am. Chem. Soc*. **1986**, *106*, 7461.
(4) Gennaro, A.; Isse, A. A.; Saveant, J.-M.;Severin, M.-G.; Vianello, E. *J. Am. Chem. Soc*. **1996**, *118*, 7190.
(5) Gennaro, A.; Isse, A. A.; Severin, M.-G.; Vianello, E.; Bhugun, I.; Saveant, J.-M. *J. Chem. Soc., Faraday Trans*. **1996**, *92*, 3963.
(6) Bhugun, I.; Lexa, D.; Saveant, J.-M. *J. Phys. Chem*. **1996**, *100*, 19981.
(7) Bhugun, I.; Lexa, D.; Saveant, J.-M.*J. Am. Chem. Soc*. **1994**, *116*, 5015.
(8) Kushi, Y.; Nagao, H.; Nishioka, T.; Isobe, K.; Tanaka, K. *J. Chem. Soc., Chem. Commun*. **1995**, 1223.
(9) Ali, M. M.; Sato, H.; Mizukawa, T.; Tsuge, K.; Haga, M.; Tanaka, K. *J. Chem. Soc., Chem. Commun*. **1998**, 249.
(10) Collin, J.-P.; Jouaiti, A.; Sauvage, J.-P. *Inorg. Chem*. **1988**, *27*, 198.

10.1021/ja001254n CCC: $19.00
Published on Web 10/21/2000

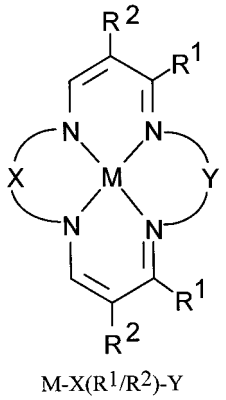

M-X(R^1/R^2)-Y

Figure 1.

and to minimize the side reactions

$$CO_2^{\cdot -} + CO_2 \rightleftharpoons CO_2 - CO_2^{\cdot -} \quad (3)$$

$$CO_2 - CO_2^{\cdot -} + e^- \rightarrow CO + CO_3^{2-} \quad (4)$$

(b) a metal complex redox catalyst with a low Lewis acidity in the oxidized form to minimize coordinative interactions between the metal center and the strongly basic $CO_2^{\cdot -}$ radical anions, and, of course, (c) anhydrous conditions to exclude that hydrogen ions favor a further reduction of protonated $CO_2^{\bullet -}$ radical anions to formate.

Toward this end, we have investigated metal chelate complexes of the general structure shown in Figure 1 with respect to their abilities to catalyze the reduction of carbon dioxide in aprotic solvents such as acetonitrile (ACN). Some preliminary experiments were also conducted in *N*,*N*′-dimethylformamide (DMF).

The redox potential and Lewis acidity of the central atom, especially in the case of the nickel complexes, can be adjusted over a wide range by the peripheral substituents R^1 and R^2, as well as the bridges X and Y,[11−16] giving rise to systematic investigations concerning the effect of these parameters on the electrocatalytic properties. Unlike positively charged macrocyclic chelate complexes of the cyclam type,[3] these complexes are neutral in the nickel oxidation state +2 resulting in a much lower tendency to interact with the negatively charged $CO_2^{\bullet -}$ radical anion. The situation with these types of complexes is similar to that described for aromatic esters and nitriles, which have proven to be selective and persistent catalysts for the reduction of CO_2 to oxalate.[4] In agreement with our expectations, the complexes shown in Figure 1 are able to catalyze the reduction of CO_2 to oxalate in ACN as well as in DMF.

There are two isomers of the macrocycles in Figure 1 with respect to the position of the substituent R^1. While the direct template synthesis of the complexes with COOEt or COMe substitution in R^2 [17] results in the trans isomer as the main product,[13,18] the cis isomer is obtained when the complexes are prepared from the free ligand (synthesized by demetalation of the copper complex[19]) and nickel salts. The following investigations were carried out with the cis isomer as depicted in Figure 1 unless otherwise stated. Because of the quite different behavior of the nickel macrocycles compared to their cyclam-type counterparts, we also describe briefly the electrochemistry of two macrocyclic cobalt chelate complexes in the presence of CO_2.

Results of Cyclic Voltammetric Investigations on Macrocyclic Nickel Chelate Complexes in the Absence and Presence of Carbon Dioxide

The various macrocyclic complexes that we have investigated with respect to their ability to catalyze the electrochemical reduction of CO_2 are listed in Table 1. The data represent average values from at least three independent experiments. In the absence of carbon dioxide, these complexes show a reversible cyclic voltammetric wave assigned to the process.

$$NiL + e^- \rightleftarrows NiL^- \qquad (E^\circ, \alpha, k_s) \quad (5)$$

This could be proven by electrolyzing the complexes under potentiostatic conditions in a cell that was equipped with a cuvette for optical or ESR spectroscopy. At the end of the electrolysis, the ESR spectra were measured in liquid nitrogen at 77 K. The ESR data for some complexes are summarized in Table 2.

The standard potentials and kinetic parameters for all complexes were obtained by subjecting experimental CVs (seven scan rates from 1 to 80 V/s) to the data-fitting routine of the DigiSim program.[23] A comparison of experimental and simulated CVs for the complexes Ni−Etn(Me/COOEt)Etn and Ni−Etn(Me/H)Tmn is displayed in Figure 2a, b, respectively.

Although the rate constants, k_s, of the charge-transfer reaction have not been corrected for double-layer effects, the picture shows, at least qualitatively, a remarkable effect of the equatorial substituents on the speed of the charge-transfer reaction. The rate constants for symmetrically bridged complexes with a COOEt or COMe group in the R^2 position range typically from 0.1 to 0.2 cm/s, but the value of k_s drops to 0.05 cm/s for Ni−Etn(Me/COOEt)Tmn where the symmetry of the complex is disturbed by introducing a trimethylene bridge. A similar deceleration of the charge-transfer reaction is achieved by removing the COOEt or COMe group in the R^2 position, and the superimposition of both effects makes k_s for Ni−Etn(Me/H)Tmn 1 order of magnitude smaller than for Ni−Etn(Me/COOEt)Etn.

In the presence of carbon dioxide, the reversibility of the cyclic voltammetric wave is lost and the cathodic peak current is enhanced. Potentiostatic electrolyses of the complexes in ACN saturated with CO_2 at potentials where only the catalytic reduction takes place yielded oxalate as the main product. These results and the very small tendency of the macrocyclic nickel(II) chelate complexes to interact with Lewis bases suggest that, within the time scale of the cyclic voltammetric experiment,

(11) Pillsbury, D. G.; Busch, D. H. *J. Am. Chem. Soc*. **1976**, *98*, 7836. Streeky, J. A.; Pillsbury, D. G.; Busch, D. H. *Inorg. Chem*. **1980**, *19*, 3148.
(12) Jäger, E.-G.; Rudolph, M.; Müller, R. *Z. Chem*. **1978**, *18*, 229.
(13) Jäger, E.-G.; Kirchhof, B.; Schmidt, E.; Remde, B.; Kipke, A.; Müller, R. *Z. Anorg. Allg. Chem*. **1982**, *485*, 141.
(14) Jäger, E.-G. In *Chemistry at the Beginning of the Third Millennium*; Fabbrizzi, L., Poggi, A., Eds.; Springer: Berlin, Heidelberg, New York, 2000; pp 103−138.
(15) Rudolph, M. Ph.D. Thesis, University of Jena, 1980.
(16) Jäger, E.-G.; Rudolph, M. *Z. Chem*. **1981**, *21*, 371.
(17) Jäger, E.-G. *Z. Chem*. **1968**, *8*, 30.
(18) Alcock, N. W.; Lin, W.-K.; Jircinato, A.; Mokren, J. D.; Corfield, P. W. R.; Johnson, G.; Novotnak, G.; Cairns, C.; Busch, D. H. *Inorg. Chem*. **1987**, *26*, 440.
(19) Jäger, E.-G. *Z. Chem*. **1968**, *8*, 470.
(20) Riley, D. P.; Busch, D. H. *Inorg. Synth.* **1978**, *23*, XVIII, 36.
(21) Renner, P. Ph.D. Thesis, University of Jena, 1977.
(22) Gennaro, A.; Isse, A. A.; Vianello, E. J. *Electroanal. Chem*. **1990**, *289*, 203.
(23) Rudolph, M.; Feldberg, S. W. *DigiSim 3.0*; Bioanalytical Systems Inc., West Lafayette, IN 47906.

Table 1. Standard Potentials and Kinetic Constants[a] for the Electrochemical Reduction of CO_2 Catalyzed by Nickel Chelate Complexes of Type 3 in ACN + 0.25 M Bu_4NClO_4

complex	$E°$ (V)	α	k_s (cm/s)	k_{et} ($M^{-1}\,s^{-1}$)	k_d ($M^{-1}\,s^{-1}$)
cis-Ni−Etn(Me/H)Tmn[b]	−2.243	0.415	0.015	9×10^3	2×10^8
cis-Ni−Etn(Me/COOEt)Etn	−2.176	0.425	0.25	1.3×10^5	2×10^6
trans-Ni−Etn(Me/COOEt)Etn	−2.163	0.42	0.25	1×10^5	1×10^6
cis-Ni−Etn(Me/COMe)Etn	−2.112	0.46	0.12	2.2×10^4	1.7×10^7
cis-Ni−Etn(Ph/COEt)Etn	−2.104	0.45	0.12	1.2×10^4	1×10^7
cis-Ni−Tmn(Me/H)Tmn[c]	−2.103	0.43	0.05	1.3×10^4	2×10^8
trans-Ni−Etn(Ph/COOEt)Etn	−2.089	0.45	0.11	9×10^3	1×10^7
cis-Ni−Etn(Me/COMe)Tmn[d]	−1.970	0.49	0.05	100	
cis-Ni−Tmn(Me/COMe)Tmn[e]	−1.880	0.48	0.1		

[a]Reactions 5−7. [b]With inclusion of reaction 8, $k_p = 1.5 \times 10^3\ M^{-1}\ s^{-1}$. [c]With inclusion of reaction 8, $k_p = 1.2 \times 10^4\ M^{-1}\ s^{-1}$. [d]Parameter not determinable from our experiments. [e]No enhancement of the cathodic peak in the presence of CO_2; only small effect in the backward scan of the CV; kinetic parameters for reaction with CO_2 could not be determined.

Table 2. ESR Data for Electrolytically Generated Nickel(I) Complexes in DMF + 0.1 M Et_4NClO_4 at 77 K

complex	$g_{\|\|}$	$g_\perp$
Ni−Etn(Me/COOEt)Etn	2.177	2.049
Ni−Etn(Me/COMe)Etn	2.174	2.051
Ni−Phn(Me/COOEt)Phn	2.107	2.022
Ni−Tmn(Me/COMe)Tmn	2.237	2.060
Ni−Etn(Me/COet)Tmn	2.220	2.066
Ni−Etn(Me/COMe)Tmn	2.222	2.057

the catalytic regeneration of the catalyst NiL in eq 5 proceeds as an outer-sphere reaction

$$NiL^- + CO_2 \underset{k_{-et}}{\overset{k_{et}}{\rightleftharpoons}} NiL + CO_2^{\bullet -} \qquad (6)$$

followed by fast dimerization reaction to oxalate

$$CO_2^{\bullet -} + CO_2^{\bullet -} \xrightarrow{k_d} C_2O_4^{2-} \qquad (7)$$

The determination of the kinetic parameters k_{et} and k_d was accomplished again by fitting experimental CVs with simulated ones. The standard potentials and the kinetic parameters k_s and α as well as the diffusion coefficients of the catalysts (typical values are $D_{NiL} = (1.0-1.2) \times 10^{-5}$ cm^2/s) used in the fitting routine as invariable quantities have been determined beforehand in the absence of CO_2. The equilibrium constant $K_{et} = k_{et}/k_{-et}$ was calculated by the DigiSim simulation program[24] from the standard potentials of CO_2 (−2.21 V vs SCE) and catalyst, respectively. All complexes were investigated in ACN at four carbon dioxide concentrations (5.35−15.7 mM) and five scan rates (0.077−1 V/s). We observed two different types of cyclic voltammograms depending on whether the complex was substituted by a COOEt or COMe group in R^2 position or by H only. We first concentrate on the complexes with R^2 = COOEt or R^2 = COMe.

Some examples of experimental and simulated CVs are shown in Figures 3−5. For all complexes, except Ni−Etn(Me/COMe)-Tmn, the experimental CVs can be simulated almost perfectly on the basis of reactions 5−7.

For the most active catalysts at low CO_2 concentrations and scan rates, the second-order character of reaction 6, i.e. the depletion of CO_2 near the electrode, results in CVs that still exhibit cathodic current peaks. In this situation, the diffusion coefficient of the CO_2 could be determined by the fitting procedure.

Unlike the other complexes with COOEt or COMe substitution in the R^2 position, the experimental CVs of the complex

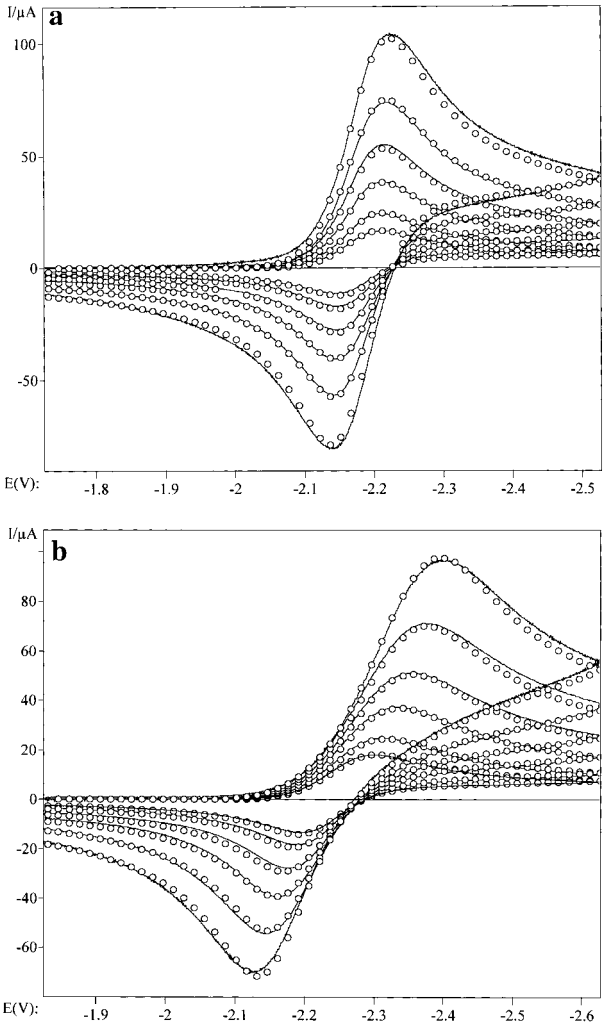

Figure 2. Comparison of experimental (—) and simulated (○) CVs for the reduction of (a) Ni−Etn(Me/COOEt)Etn and (b) Ni−Tmn(Me/H)Etn in ACN + 0.25 M Bu_4NClO_4 at scan rates of 1, 2, 5, 10, 20, and 40 V/s.

Ni−Etn(Me/COMe)Tmn cannot be interpreted satisfactorily on the basis of reaction schemes 5−7 over the whole range of scan rates and CO_2 concentrations. The agreement between experimental and simulated CVs in Figure 5 becomes worse the higher the CO_2 concentration and/or the slower the scan rates in the experiments. The disagreement concerns mainly the backward scan in the CV, which is much smaller than it should be according to the above reaction scheme. The fitting routine tries to compensate this effect by increasing the rate constant of the

(24) Rudolph, M. In *Physical Chemistry: Principles, Methods and Applications*; Rubinstein, I., Ed.; Marcel Dekker: New York 1995.

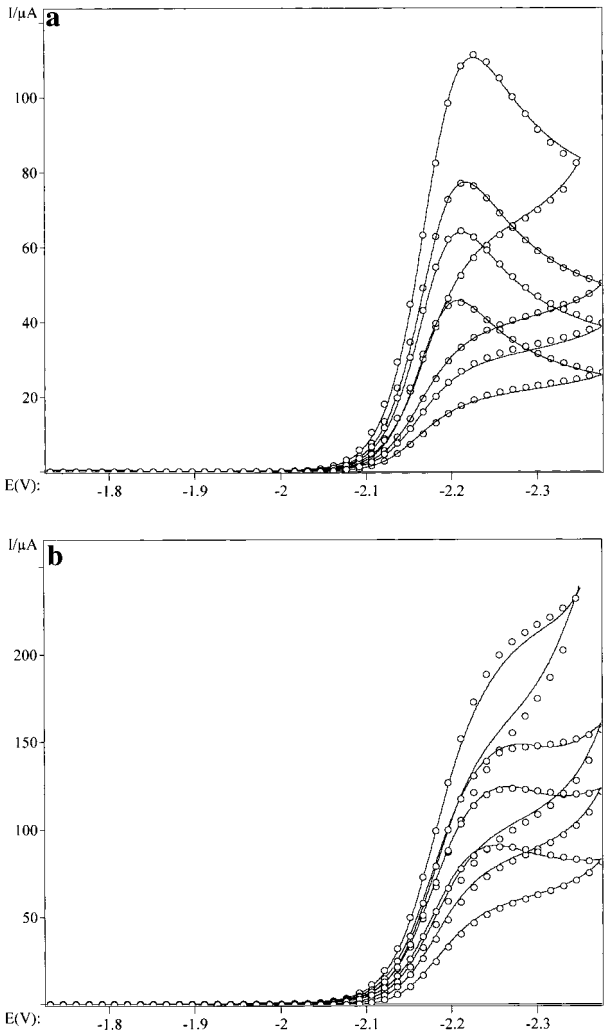

Figure 3. Comparison of experimental (—) and simulated (○) CVs for the reduction of Ni−Etn(Me/COOEt)Etn in ACN + 0.25 M Bu_4NClO_4 at CO_2 concentrations of 5.35, 7.73, 10.4, and 15.7 mM: (a) v = 0.077 V/s; (b) v = 1 V/s.

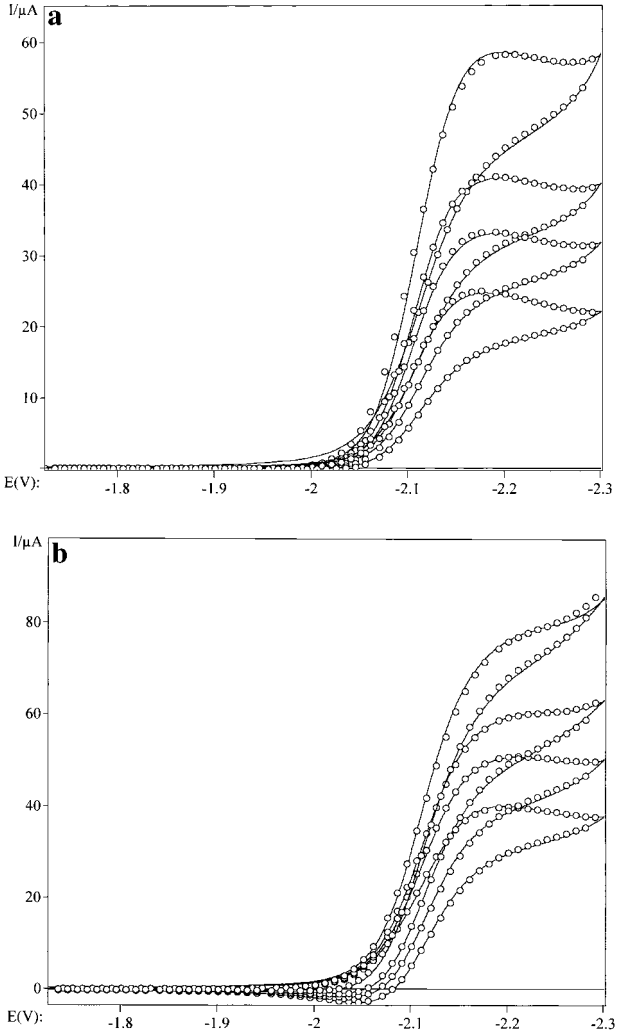

Figure 4. Comparison of experimental (—) and simulated (○) CVs for the reduction of Ni−Etn(Ph/COOEt)Etn in ACN + 0.25M Bu_4NClO_4 at CO_2 concentrations of 5.35, 7.73, 10.4 and 15.7 mM, (a) v = 0.077 V/s and (b) v = 1 V/s.

dimerization reaction 7 up to unrealistically high values (beyond the limit of diffusion control). Attempts to simulate this behavior by taking some possible follow-up reactions such as (3) or $NiL + CO_2^{\bullet -} \rightarrow$ products, $NiL^- + CO_2 \rightarrow$ products, into account did not succeed. However, the assumption that the complex, in either nickel oxidation state +1 or +2, will be deactivated by follow-up reactions with CO_2 or the $CO_2^{\bullet -}$ radical anion is supported by the electrolyses experiments. Ni−Etn(Me/COMe)-Tmn is the only complex with COOEt or COMe substitution in the R^2 position where the electrolysis current quickly drops toward zero in the presence of CO_2 (see next section describing the results of electrolyses experiments).

In the case of the complexes without COOEt or COMe substitution in the R^2 position, the existence of a follow-up deactivation reaction becomes visible even in the time scale of the cyclic voltammetric experiments. The standard potential of the complex Ni−Tmn(Me/H)Tmn is almost identical with that of Ni−Etn(Ph/COOEt)Etn. Thus, a similar catalytic activity could be expected. However, a comparison of Figure 4a and 6a reveals that the enhancement of the catalytic current for Ni−Tmn(Me/H)Tmn is much smaller and only slightly dependent on the CO_2 concentration.

In contradiction to the lower catalytic activity are the peak-shaped CVs measured for Ni−Tmn(Me/H)Tmn with scan rates of 1 V/s in the presence of CO_2. This contradiction cannot be overcome within the framework of the above mechanism, but the shape and slight CO_2 dependence of the CVs can be simulated, even quantitatively, by adding the deactivation reaction

$$NiL^- + CO_2 \xrightarrow{k_p} P \qquad (8)$$

to reactions 5−7. It is noteworthy that the value k_{et} determined by the fitting routine for the catalyst Ni−Tmn(Me/H)Tmn on the basis of the extended reaction scheme was exactly as expected from the standard potential. However, almost the same k_{et} value was obtained for Ni−Tmn(Me/H)Etn, which is the complex with the most negative standard potential of all investigated catalysts and the only one with a standard potential more negative than that of CO_2. Any trial to fit the behavior of this complex with an expected rate constant $k_{et} > 10^5\ M^{-1}\ s^{-1}$ failed. Thus, it remains unclear why the homogeneous electron transfer would not be accelerated by a smaller difference in the standard potentials of complex and carbon dioxide, respectively.

To see how the catalytic activity of the nickel complexes compares with that described for aromatic nitriles and esters in DMF,[4] we have also investigated the catalytic activity of some

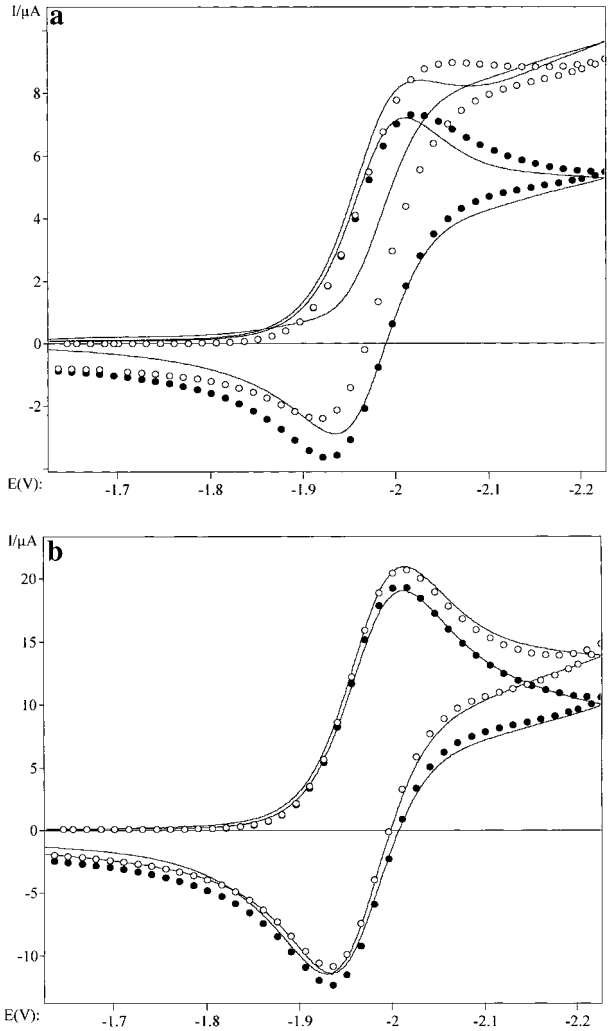

Figure 5. Comparison of experimental (—) and simulated CVs (open and filled circles) for the reduction of Ni−Etn(Me/COMe)Tmn in ACN + 0.25 M Bu_4NClO_4 at CO_2 concentrations of 5.35 (●) and 15.7 mM (○): (a) $\upsilon = 0.125$ V/s; (b) $\upsilon = 1$ V/s.

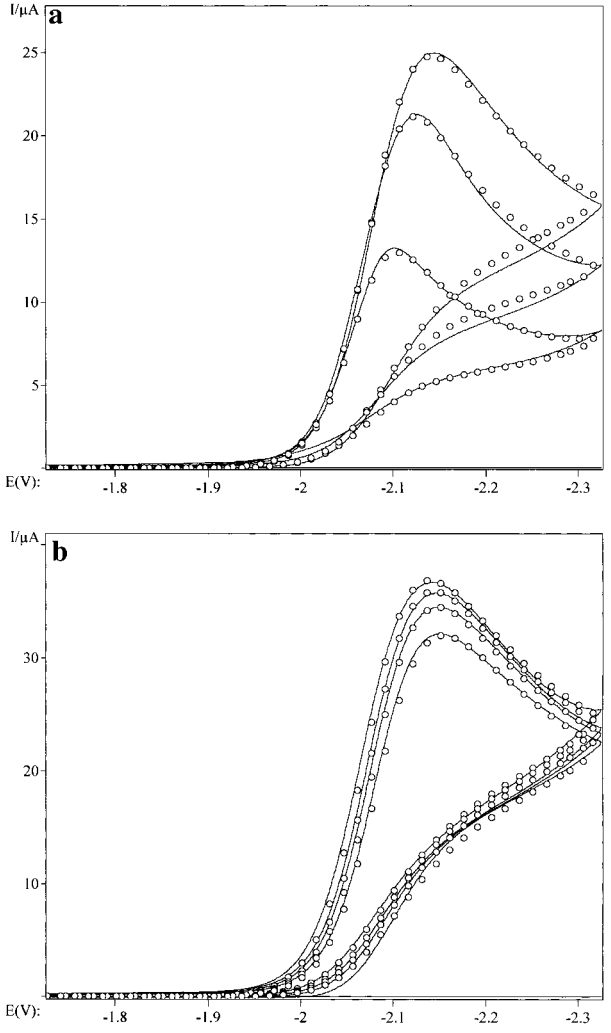

Figure 6. Comparison of experimental (—) and simulated (○) CVs for the reduction of Ni−Tmn(Me/H)Tmn in ACN + 0.25 M Bu_4NClO_4: (a) $\upsilon = 0.077$ V/s, $[CO_2]$ =7.73, 10.4, and 15.7 mM; (b) $\upsilon =$ 0.5V/s, $[CO_2] =$ 5.35,7.73, 10.4, and 15.7 mM.

of our complexes in DMF. The results can be summarized as follows. The cyclic voltammetric reduction of the complexes in DMF in the presence of CO_2 can be described in terms of the reaction equations 5−7 again, but the rate constant of the homogeneous electron-transfer reaction k_{et} is decreased by a factor of ∼2.5 compared to the value in ACN.

Results of Preparative-Scale Electrolyses Experiments

The results of the preparative-scale electrolyses for the various complexes are summarized in Table 3. The electrolyses have been conducted under potentiostatic conditions. The potential of the working electrode was always 100 mV more negative than the half-wave potential of the corresponding complex. Nevertheless, the charge consumed by the individual complexes per hour does not reflect the real differences in their catalytic activity due to an *IR* drop that makes the real potential of the working electrode less negative the higher the current (catalytic activity) of the complex. Consequently, the effective working potential was somewhere in the ascending part of the current curve but not yet in the plateau especially for the complexes Ni−Etn(Me/COOEt)Etn and Ni−Etn(Me/COMet)Etn.

The data in Table 3 and the time dependence of the electrolysis current depicted in Figure 7 reveal that (similar to the results of the cyclic voltammetric experiments) the behavior of the complexes in the electrolyses experiments is strongly effected by the substituent in the R^2 position.

Table 3. Results of Preparative-Scale Electrolyses for Various Macrocyclic Nickel Complexes (1.5×10^{-5} Mol Complex in 15 mL of ACN +0.25 M Bu_4NClO_4 Saturated with CO_2

complex	catalytic cycles	catalytic cycles/hour	oxalate faradaic yield (%)	CO faradaic yield (%)
Ni−Etn(Me/COOEt)Etn	130	55	≥98	<1
	300	52	95	2
	750	43	90	5
Ni−Etn(Me/COMe)Etn	100	40	83	<1
	250	35	78	3
Ni−Etn(Ph/COOEt)Etn	80	32	60	<1
	150	30	51	6
Ni−Etn(Me/COMe)Tmn	4	*a*	94	<1
	10	3	88	10
Ni−Etn(Me/H)Tmn	15	6	25	*c*
Ni−Tmn(Me/H)Tmn	4	*a*	*b*	*c*

[a]Fast deactivation reaction; electrolysis was terminated after ∼15 min (current dropped to ≤10% of initial value). [b]Total amount of oxalate very small (<1 mg) and hardly reproducible. [c]Not determined.

Obviously, the complexes with COOEt or COMe substitution in the R^2 position are not only more active but also more

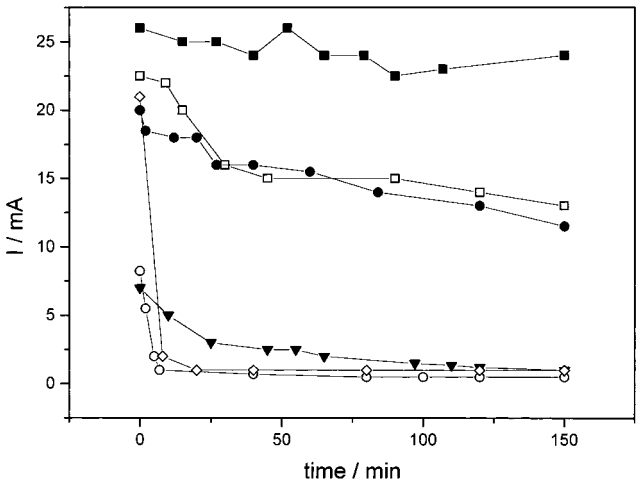

Figure 7. Current as function of time during electrolysis of nickel macrocycles in ACN + 0.25 M Bu_4NClO_4 saturated with CO_2: Ni−Etn(Me/COOEt)Etn (■); Ni−Etn(Me/COMe)Etn (□); Ni−Etn(Ph/COOEt)Etn (●); Ni−Etn(Me/COMe)Tmn (○); Ni−Etn(Me/H)Tmn (▼); Ni−Tmn(Me/H)Tmn (◇).

persistent than their unsubstituted counterparts. To visualize the differences in the behavior of the COOEt- or COMe-substituted complexes, it was necessary to stress the catalysts in long-time electrolyses while oxalate was the only detectable product with a faradaic yield; greater than 95% in short-time electrolyses (∼5 catalytic cycles; defined as n_e/n_c, where n_e denotes the molar number of electrons consumed by n_c mol of the catalyst.)

The best catalyst in all categories is Ni−Etn(Me/COOEt)-Etn. The formation of oxalate occurred quantitatively if ≤125 mM of electrons were consumed by 1 mM catalyst. Moreover, there is no visible loss of activity; i.e., the electrolysis current and the orange color of the complex in ACN remain unchanged over several hours. A significant loss of the catalytic activity became visible only after 750 catalytic cycles, but even then the faradaic yield of oxalate was still 90% while only 5% could be found in the form of CO. The other complexes showed symptoms of a partial loss of activity much earlier. This statement also holds true of electrolyses performed with benzonitrile as the redox catalyst. Benzonitrile has proven to be a fairly persistent and selective electrocatalyst for oxalate production in CO_2-saturated DMF,[4] but in test electrolyses that we have carried out in CO_2 saturated ACN, the catalyst started on a very high current level (comparable with Ni−Etn(Me/COOEt)Etn) but the electrolysis current dropped to a few milliamperes within 1 h. Thus, the benzonitrile catalyst accomplished only ∼45 catalytic cycles in 150 min.

The complexes Ni−Etn(Ph/COOEt)Et and Ni−Etn(Me/COMe)Etn exhibit a relatively moderate decay of the electrolysis current and remain active over several hours. After ∼40 catalytic cycles, the orange color of the solution of Ni−Etn(Me/COMe)-Etn in ACN becomes darker and darker and finally turns to brown. Also the faradaic yield of oxalate seems to decrease the more catalytic cycles the complexes underwent. Both observations point to slow side and/or decomposition reactions the complex undergoes during electrolysis. Nevertheless, the faradaic yield obtained by Ni−Etn(Me/COMe)Etn in long-time electrolyses was always higher than that of Ni−Etn(Ph/COOEt)-Etn albeit no visible change in the color of the complex was observed when the latter complex being electrolyzed. The lack in the charge balance for both complexes has not yet cleared up. While hydrogen and formate could never be detected, an increasing concentration of CO was found in the gas phase of the electrolysis cell the longer the time of the electrolysis. But the amount of CO compensates the lack in the charge balance only to a small extent. Unlike the other complexes with R^2 = COOEt or R^2 = COMe, the complex Ni−Etn(Me/COMe)Tmn was quickly deactivated by CO_2. The complex started with a relatively low current that dropped to a value of ∼1 mA after a few catalytic cycles without any visible change in the color of the complex solution. A similar behavior was also observed for Ni−Tmn(Me/H)Tmn. The reduction potential of this complex is close to that of Ni−Etn(Ph/COOEt)Etn. Indeed, the electrolysis current for both complexes is very similar at the very beginning but that of Ni−Tmn(Me/H)Tmn drops to zero after only two or three catalytic cycles. Parallel to the current decay, the color of the solution turns from olive-green (the typical color of the complexes with sixteen-membered macrocycles but without COOEt or COMe substitution) to orange. The total amount of oxalate was <1 mg and could not be reproduced well so that no faradaic yield is reported in Table 3.

Interestingly, the complex Ni−Etn(Me/H)Tmn with the most negative reduction potential of all investigated complexes starts on a relatively low current level. The activity of the complex at the very beginning of the electrolysis is not higher than that of Ni−Etn(Me/COMe)Tmn, which is the complex with the least negative reduction potential. However, unlike Ni−Tmn(Me/H)-Tmn, the current decay proceeds slower and the electrolyte turns to orange only in the vicinity of the working electrode while the bulk remains yellowish-green. Since the complex remains active for a longer time (albeit on a very low level), the total amount of oxalate that was found at the end of the electrolysis was ∼1 order of magnitude higher than that for Ni−Etn(Me/COMe)Tmn and Ni−Tmn(Me/H)Tmn but only ∼20% of the applied current led to oxalate.

Results of Cyclic Voltammetric Investigations on Macrocyclic Cobalt Chelate Complexes in the Absence and Presence of Carbon Dioxide

In addition to the catalytically active macrocyclic nickel complexes, two cobalt macrocycles have been examined with respect to their ability to react with carbon dioxide. Although no catalytic activity could be observed, the cyclic voltammetric reduction of the cobalt(II) complexes does strongly change in the presence of CO_2. The experiments point at a strong but kinetically labile bonding of CO_2 by the cobalt(I) species and can be interpreted in terms of the following square scheme

$$\mathrm{CoL}^- + \mathrm{CO_2} \underset{k_f/K_{CO_2}}{\overset{k_f}{\rightleftharpoons}} \mathrm{CoLCO_2}^-$$

$$(E_1^\circ, k_{s_1}, \alpha_1) \quad -e^- \downdownarrows + e^- \qquad -e^- \downdownarrows + e^- \ (E_2^\circ, k_{s_2}, \alpha_2)$$

$$\mathrm{CoL} + \mathrm{CO_2} \overset{k_D}{\longleftarrow} (\mathrm{CoLCO_2}) \qquad (9)$$

There is, however, no evidence for the existence of a CoL−CO_2 adduct in the oxidation state Co(II). The reoxidation of the corresponding Co(I) adduct, CoL−$CO_2^{\cdot -}$, appeared as a totally irreversible charge-transfer process in the backward scan of the CV even when running two cycles at scan rates up to 1000 V/s. On account of the well-known coupling between standard potential and rate constant for an irreversible heterogeneous electron transfer, it is principally not possible to determine these parameters from cyclic voltammetric experiments. Thus, the values of E_2° and k_{s2} have no significance and were used just to enable the program to fit the shape of the

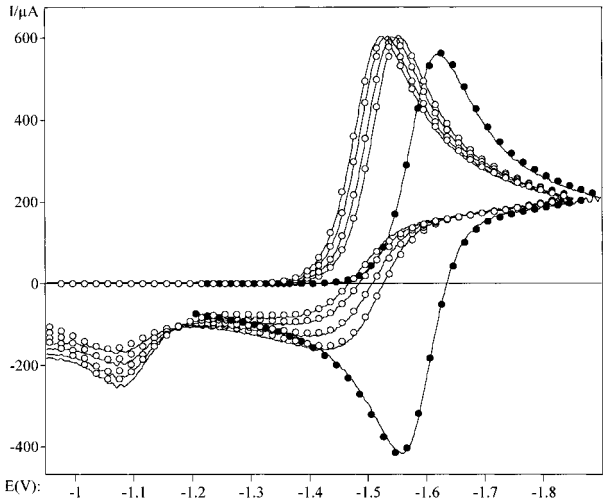

Figure 8. Comparison of experimental (—) and simulated CVs for the reduction of Co−Etn(Me/COOEt)Etn in ACN + 0.25 M Bu_4NClO_4 in the absence (●) and presence (○) of carbon dioxide (34, 70, 157, and 295 mM) at $\upsilon = 400$ V/s.

experimental CVs. It was further assumed that the dissociation reaction of the CoL(II)−CO_2 adduct is under diffusion control ($k_D > 10^{10}$ M^{-1} s^{-1}) and α_1 was set to 0.5 since the observed heterogeneous rate constant, k_{s_1}, measured in the absence of CO_2 was ≥1 cm/s. A comparison of simulated and experimental CVs for the complex Co−Etn(Me/COOEt)Etn is shown in Figure 8.

The values retrieved by the fitting procedure are as follows: $E_1^\circ = -1.587$ V, $K_{CO_2} = 2200$ M^{-1} and $k_f = 1.8 \times 10^8$ M^{-1} s^{-1} for the complex Co−Etn(Me/COOEt)Etn and $E_1^\circ = -1.510$ V, $K_{CO_2} = 600$ M^{-1} and $k_f \sim 1 \times 10^8$ M^{-1} s^{-1} for Co−Etn(Me/COMe)Etn. However, the quality of the fits for the latter complex was not so good due to the uncertainty in the complex concentration resulting from the low solubility of Co−Etn(Me/COMe)Etn in ACN. Also, the complex produced some additional charging current that could not be corrected for by subtracting the baseline of the background electrolyte. This could be a reason for a drift in the k_f value from 6×10^7 to 1.3×10^8 M^{-1} s^{-1} with increasing CO_2 concentrations.

It is noteworthy that the rate constants k_f measured for our complexes are of the same order of magnitude as those obtained for cationic tetraazamacrocycles with a similar reduction potential although their equilibrium constants are usually 2 orders of magnitude higher.[25−27] For instance, the reduction potentials of the complexes $Co^{II}DMD^{2+}$ and $Co^{II}HMD^{2+}$ (see the original papers) are −1.51 and −1.38 V (vs SCE), respectively, while the equilibrium constant for both complexes is $K_{CO_2} \approx 10^5$ M^{-1}. Also, the rate constants reported for both complexes differ only slightly ($k_f = 3.6 \times 10^8$ and $k_f = 1.8 \times 10^8$ M^{-1} s^{-1}, respectively). It is surprising that the positively charged complex $Co^{I}HMD^{+}$ has a higher affinity toward the acidic CO_2 molecule than the negatively charged complex Co^{I}−Etn(Me/COOEt)Etn^-, which has the more negative reduction

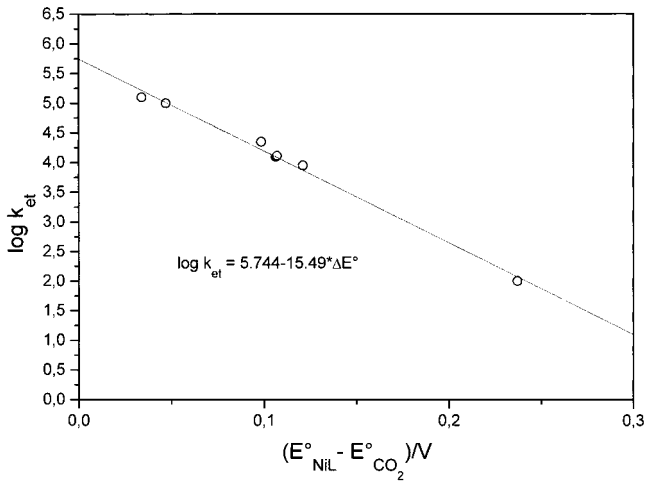

Figure 9. Variation of the rate constant of electrontransfer, k_{et}, with the standard free energy of reaction 6 in ACN + 0.25 M Bu_4NClO_4.

potential. In principle, this can be only understood by suspecting a remarkable charge transfer from the cobalt(I) to the bound CO_2 so that the adduct is best interpreted as a $Co^{II}L-CO_2^-$ species. The higher affinity comes then from the higher Lewis acidity of the cationic $Co^{II}HMD^{2+}$ complex toward the strongly basic $CO_2^{\bullet-}$ radical anion. Such a charge transfer was not only predicted theoretically[32] but also found experimentally.[28] Splitting the adduct formation in two subsequent reactions, $Co^{I}L^- + CO_2 \rightleftarrows Co^{II}L + CO_2^{\bullet-}$ and $Co^{II}L + CO_2^{\bullet-} \rightleftarrows Co^{II}L-CO_2^{\bullet-}$ reveals that a catalytic reaction, i.e., the dissociation of the CO_2 adduct into Co(II) and $CO_2^{\bullet-}$, is a strongly disfavored process for such cobalt complexes. The equilibrium constant of the second reaction is 10^{14} for Co−Etn(Me/COOEt)Etn (and correspondingly higher for $Co^{II}DMD^{2+}$ and $Co^{II}HMD^{2+}$) because the equilibrium constant of the first reaction calculated from the difference of the standard potentials is $\sim 2 \times 10^{-11}$ and the product of both equilibrium constants equals $\sim 2 \times 10^3$.

Discussion

Studying the rate constants of the homogeneous electron transfer compiled in Table 1 evokes the question of whether k_{et} depends on the standard potential as predicted by the Marcus equation for an outer-sphere mechanism or whether there is any evidence for a direct interaction between the catalyst and the carbon dioxide. Figure 9 shows how the homogeneous rate constants k_{et} vary with the standard free energy of reaction 6, ΔG° (eV) = ($E^\circ_{NiL} - E^\circ_{CO_2}$) (V).

The plot can be described in terms of the linear equation log $k_{et} = 5.75-15.5 \times \Delta G^\circ$/(eV). The slope of the plot indicates that the rate constant changes by 1 order of magnitude if the standard potential varies by ∼64 mV instead of 120 mV as expected for a simple electron-transfer reaction in a driving force range around zero where the symmetry factor is close to 0.5. A similar observation has been published recently for the CO_2 reduction catalyzed by aryl esters in DMF in the low driving force zone (i.e., aryl esters with standard potentials similar to those of the macrocyclic nickel complexes described in this paper).[4] Also the value of the rate constant extrapolated for $\Delta G^\circ = 0$, $k_{et} \sim 5.6 \times 10^5$ M^{-1} s^{-1}, is very close to the value published there taking into account that the activity of our complexes is ∼2.5 times smaller in DMF. Following the argument of the above paper, we can conclude that the 1/(64 mV) slope points to an inner-sphere mechanism involving two

(25) Fujita, E.; Creutz, C.; Sutin, N.; Szalda, D. J. *J. Am. Chem. Soc.* **1991**, *113*, 343.
(26) Ogata, T.; Yanagida, S.; Brunschwig, B. S.; Fujita, E. *J. Am. Chem. Soc.* **1995**, *117*, 6708.
(27) Ogata, T.; Yanagida, S.; Brunschwig, B. S.; Fujita, E. *Energy Convers. Manage.* **1995**, *36*, 669.
(28) Fujita, E.; Furenlid, L. R.; Renner, M. W. *J. Am. Chem. Soc.* **1997**, *119*, 4549.
(29) Wolf, L.; Jäger, E.-G. *Z. Anorg. Allg. Chem.* **1966**, *346*, 76.
(30) Schade, W.; Jäger, E.-G.; Müller, K.; Seidel, D. *J. Prakt. Chem.* **1989**, *331*, 559.
(31) Honeybourne, C. L. *Tetrahedron* **1973**, *29*, 1549.
(32) Salaki, S.; Dedieu, A. *Inorg. Chem.* **1987**, *26*, 3278.

successive steps

$$NiL^- + CO_2 \underset{k_{b_1}}{\overset{k_{f_1}}{\rightleftharpoons}} NiLCO_2^- \quad (10)$$

$$NiLCO_2^- \underset{k_{b_2}}{\overset{k_{f_2}}{\rightleftharpoons}} NiL + CO_2^{\bullet -} \quad (11)$$

where the observed overall rate constant k_{et} in reaction 6 can be represented by the rate constants of the individual steps (10 and 11) according to

$$k_{et} = \frac{k_{f_1} k_{f_2}}{k_{b_1} + k_{f_2}} \quad (12)$$

In fact, any simulation performed on the basis of reactions 10 and 11 instead of reaction 6 produced identical results if the rate constants k_{f_1}, k_{f_2}, and k_{b_1} were chosen to fulfill eq 12 and if

$$K_1 K_2 = K_{et} = \exp\left[\frac{F}{RT}(E^\circ_{CO_2} - E^\circ_{NiL})\right] \quad (13)$$

It might even be possible that the nature of the interactions between the CO_2 molecule and the metal complex is similar to that reported for the aryl esters.[4] For the latter compounds, the electron transfer was proposed to proceed by coordinating a CO_2 molecule on the carbonyl group where the unpaired electron was assumed to be localized in the reduced aryl ester. Since all our complexes with carbonyl or ester groups in the R^2 position are catalytically more active than those without such groups, it seems possible that the higher activity results simply from the ability of COOEt or COMe groups to promote the electron transfer between the catalyst and the carbon dioxide. On the other hand, a detailed simulation of ESR- and visible spectroscopic data indicates that the spin density of the unpaired electron is mainly localized at the metal center.[15,16] Thus, it is more likely that a labile metal−carbon bond is formed due to the attack of the electrophilic CO_2 at the nucleophilic metal center of the reduced complex. The observed ~1/(60 mV) slope experimentally found for k_{et} can then be explained by assuming that the rate constant for the dissociation of the $NiLCO_2^{\bullet -}$ adduct into the products NiL and $CO_2^{\bullet -}$ is slower than the rate constant for the dissociation into the reactants NiL^- and CO_2. In other words $k_{f_2} \ll k_{b_1}$ so that $k_{et} = K_1 k_{f_2}$ and the 1/(60 mV) line results from a linear free energy relationship between k_{et} and $K_1 = k_{f_1}/k_{b_1}$. An ideal (1/60 mV) slope would require that the variation of K_1 parallels the variation of E°_{NiL} and that k_{f_2} is the same for each complex. The first assumption is likely to be true because the standard potential reflects the electron density of the metal center which causes the electrophilic attack of the CO_2. The second assumption holds true because K_{et} is <1 for all complexes shown in Figure 9 and because of the high kinetic lability of a d^9 nickel(I) complex provided the rate constant k_{b_2} of the adduct formation between $Ni^{II}L$ and $CO_2^{\bullet -}$ is not faster than that between the isoelectronic $Co^{I}L^-$ complex and CO_2 (see previous section).

The other requirement, namely, that k_{f_2} is approximately the same for each complex, is more unlikely. However, it was demonstrated in the above mentioned paper[4] that a linear relationship between log k_{et} and $E^\circ_{NiL} - E^\circ_{CO_2}$ can also be expected for not constant k_{f_2} values. In this case, the slope of the line lies between 1/(60 mV) and 1/(120 mV) if the standard free energies of both reactions 10 and 11 are proportional to the standard free energy of the overall reaction, ΔG° (eV) = $(E^\circ_{NiL} - E^\circ_{CO_2})$ (V).

Within the framework of the above model, there is no explanation for the differences in the rate constant of the dimerization reaction 7 retrieved for the individual complexes. Also, the values obtained in our experiments are 1−2 orders of magnitude smaller than the value $k_d \sim 10^8$ M^{-1} s^{-1} reported in the literature[4] for DMF. This value is a correction for the previously published rate constant $k_d \sim 10^7$ M^{-1} s^{-1}.[33] The simplest solution for this discrepancy would be to assume that the complexes undergo a small shift in the reduction potential to more negative potentials in the presence of CO_2. To give an example, a shift in the standard potential of ~8 mV in a negative direction would be enough to move the value of k_d from ~10^6 to 5×10^8 M^{-1} cm^{-1}. The example illustrates that the effect of k_d on the cyclic voltammetric curves is small but it could be reproduced in several independent experiments. Of course, the virtual shift of the standard potential may also result from a change of the diffusion coefficients so that the ratio $D_{NiL}/D_{NiL}-$ becomes >1 while the simulation of the CVs was performed with $D_{NiL}/D_{NiL}- = 1$. The only reason one could envision for a change of this ratio in the presence of carbon dioxide is an enlarged solvation sphere of the nickel(I) species resulting from the attraction of polarizable CO_2 molecules by the negative charge of the complex. Whatever the real nature of the follow-up reaction that leads to the dimerization of the $CO_2^{\bullet -}$ radical anions, it should have only a small effect on the observed overall rate constant k_{et} and the differences in the standard deviations of fits obtained for alternative mechanisms are too small as to justify more speculations.

Another striking point in our investigations is the remarkable difference in the cyclic voltammetric behavior of complexes with and without COOEt or COMe substitution in the R^2 position in the presence of carbon dioxide. The observations reported in this paper parallel our experiences with cobalt and iron complexes of both types with respect to the catalytic activation of dioxygen.[14] In all these cases, only the acetyl- or carbethoxy-substituted complexes exhibit a sufficient stability while the unsubstituted complexes seem to be sensitive toward attacks of electrophilic agents. MO calculations[31] predict a remarkable amount of negative charge localized at the carbon atom in the R^2 position if the complexes are not substituted there. Undoubtedly, this effect is even larger for the negatively charged nickel(I) complexes so that an electrophilic attack of the CO_2 molecule at the unprotected nucleophilic C-atom in the R^2 position could be responsible for the observed loss of catalytic activity for Ni−Tmn(Me/H)Tmn and Ni−Etn(Me/H)-Tmn. The result of such an attack could be a complex with COOH substitution in the R^2 position that is insoluble in organic solvents such as acetonitrile.[29]

Although the deactivation reactions of the complexes have not yet been investigated in detail, we have compared cyclic voltammograms of the complex Ni−Tmn(Me/H)Tmn with those measured at the end of the electrolysis under CO_2 and argon atmosphere. The CVs are shown in Figure 10.

The full line marks the CV of the olive-green solution of the complex in ACN under an argon atmosphere. The solvent was then saturated with CO_2 and electrolyzed for 30 min so that the solution turned to orange. The curve emphasized by the open circles shows the CV obtained at this state while the filled circles mark the curve obtained after removing the CO_2 by bubbling argon through the solution. Unlike the original complex, the species obtained after electrolysis shows no significant enhancement of the cathodic peak current under a CO_2 atmosphere (○);

(33) Lamy, E.; Nadjo, L.; Saveant, J.-M. *J. Electroanal. Chem.* **1977**, *78*, 403.

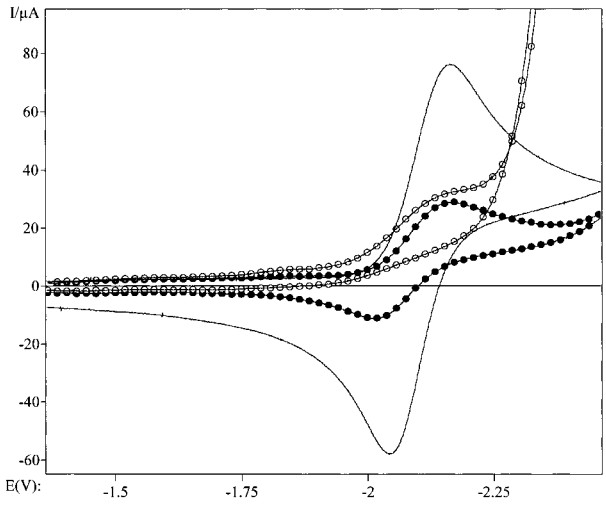

Figure 10. Cyclic voltammetric curves of Ni−Tmn(Me/H)Tmn in ACN + 0.25 M Bu_4NClO_4. (−) CV of 1 mM of the complex in the absence of CO_2; (○) CV obtained after electrolyzing the complex for 30 min under CO_2 atmosphere; (●) same as before after removing the CO_2 by bubbling argon.

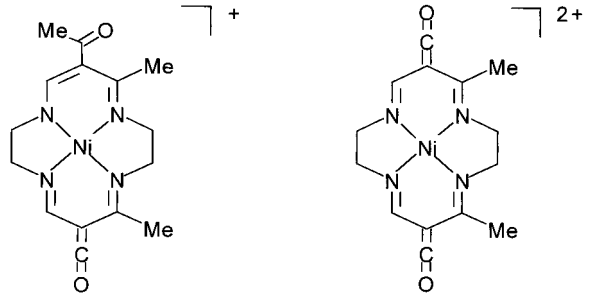

Figure 11.

the potential of the reduction peak is almost identical with that of the original complex but the reoxidation peak has drifted to 30 mV more positive potentials and the height of the cathodic peak amounts only to one-third of the original peak height. These observation are in keeping with the reaction schemes 5−7 and 8.

A examination of the results of the preparative-scale electrolyses experiments (see Results section) also reveals a significant difference in the current efficiency of the complexes Ni−Etn(Me/COOEt)Etn and Ni−Etn(Me/COMe)Etn. The current yield obtained for Ni−Etn(Me/COOEt)Etn was practically 100% while that of Ni−Etn(Me/COMe)Etn was distinctly smaller and seems to decrease the longer the electrolysis time. Also the color of the COMe-substituted complex in ACN changed from orange to brown in the course of the electrolysis. We know that the chemical properties of both complexes are quite similar in many respects, but *one* striking difference has been observed in their mass spectroscopic fragmentation:[30] In the case of Ni−Etn(Me/COMe)Etn, the CH_3 group is readily split off from the acetyl substituent R^2, resulting in the fragment cations shown in Figure 11 with nickel in the oxidation state +2 and a monoanionic or neutral "cyclidene-like" ligand.

The corresponding fragments appear with a relative intensity of 74 and 20% in the mass spectra of Ni−Etn(Me/COMe)Etn (compared to the base peak of the molecular ion signal). In contrast to this, the ethoxycarbonyl-substituted complex Ni−Etn(Me/COOEt)Etn yielded only 12 and 8% of these fragmentation products under exactly the same conditions and no other fragments were found with a intensity higher than 12%. Moreover, the acetyl-substituted complexes readily undergo decarbonylation reactions,[11] and one makes good use of this fact for preparing unsubstituted macrocyclic complexes such as Ni−Tmn(Me/H)Tmn or Ni−Etn(Me/H)Tmn, which are not amenable to template reactions.[20] The formation of the cations in Figure 11 points at a favored decomposition pathway that acetyl-substituted macrocyclic complexes undergo under mass spectroscopic conditions. Therefore, it seems possible that instead of reaction 11 the decomposition of the $NiLCO_2^-$ adduct occurs by splitting off a methyl group from the acetyl substituent. While the $CH_3^{\bullet}$ radical could be stabilized by forming acetate with the $CO_2^{\bullet-}$ radical anion, the remaining nickel complexes would be similar to those in Figure 11 but neutral with the nickel in either oxidation state +1 or 0, depending on whether such an reaction occurred to only one or both of the acetyl substituents. However, we have not tried to isolate the complexes in Figure 11 or the corresponding neutral species. Thus, we have no experimental evidence for this assumption.

Conclusions

The macrocyclic nickel complexes in Figure 1 with R^2 = COOEt or COMe and Y=Y=Etn are the first metal complexes that are remarkably selective and persistent homogeneous catalysts for the electrochemical reduction of CO_2 to oxalate. The variation of the rate constants for the generation of $CO_2^{\bullet-}$ anions by electron transfer from these complexes does not speak for a simple outer-sphere process but bears a strong resemblance with what happens when anion radicals of aromatic esters and nitriles react with carbon dioxide. With a homogeneous electron-transfer rate constant of $\sim 10^5$ $M^{-1}s^{-1}$, the complex Ni−Etn-(Me/COOEtn)Etn has proven to be the most active metal complex electrocatalyst for the electrochemical reduction of CO_2 yielding selectively oxalate that has been reported so far. The long-time activity of this catalyst in preparative-scale electrolyses experiments was better than that of any other homogeneous redox catalyst for oxalate production including aromatic esters and nitriles. Complexes without COOEt or COMe groups in the R^2 position are deactivated in the oxidation state +1 by carbon dioxide in a reaction that is first order with respect to CO_2. Consequently, in contrast to the expectation that the catalytic activity grows the more negative the reduction potential, the catalytic properties of the complexes deteriorate when removing the electron-withdrawing groups in the R^2 position.

Experimental Section

Chemicals. Acetonitrile (Merck, p.a. grade) was distilled twice from sodium hydride, phosphorus pentoxide, and finally calcium hydride. The purified product was stored under an argon atmosphere. DMF (Sigma-Aldrich, p.a. grade) was dried over anhydrous sodium carbonate for several days. It was then fractionally distilled under reduced pressure under argon. The final distillation was carried out over neutral alumina (Merck, active grade 1) activated overnight at 350 °C under vacuum. The solvent was stored under argon atmosphere protected from light. Tetra-*N*-butylammonium perchlorate (Fluka, p.a. grade) was recrystallized from methanol and dried under vacuum over phosphorus pentoxide. Carbon dioxide (99.998%) was supplied by Linde. ACN and DMF solutions containing various concentrations of CO_2 were prepared by saturating the solvent with appropriate mixtures of CO_2 and argon. The CO_2 concentration was calculated from the saturation concentration of CO_2 in the solvent[22] and the partial pressure of CO_2 in the gas mixture produced from mixing argon and CO_2 streams of well-defined flow rates. The content of CO_2 in the gas mixture was determined by gas chromatography. The COOEt- and COMe-substituted

macrocyclic nickel and cobalt complexes were prepared as described in the literature,[17,20,21] recrystallized from acetonitrile and dried under vacuum. The synthesis of the non COOEt- or COMe-substituted complexes was carried out according to Riley and Busch.[20] All complexes were characterized by H NMR and mass spectroscopy.

Instrumentation and Procedures. 1. Cyclic Voltammetry. The cyclic voltammetric measurements were made with a home-built computer-controlled instrument based on the DAP-3200a data acquisition board (Datalog Systems) as well as with the Autolab PG Stat 20 (Metrohm). The experiments were performed in a three-electrode cell under a blanket of solvent-saturated argon−CO_2 mixtures. The ohmic resistance, which had to be compensated for, was obtained by measuring the impedance of the system at potentials where the faradaic current was negligibly small. Background correction in high-speed cyclic voltammetric experiments was accomplished by subtracting the current curves of the blank electrolyte (containing the same concentration of supporting electrolyte) from the experimental CVs. The reference electrode was a Ag|AgCl electrode in acetonitrile containing 0.25 M tetra-*N*-butylammonium chloride, but for convenience, all potentials were finally referenced to the SCE throughout this paper. The working electrode for investigating the macrocyclic nickel complexes in the presence of CO_2 at very negative potentials was a mercury drop that was hung on a gold disk of ∼0.5 mm diameter. The drops were produced by the CGME instrument (Bioanalytical Systems, Inc.,West Lafayette, IN) and their radius (∼0.042 cm) was determined by comparing the capacity of the electrode with that measured for a 1.6-mm gold disk electrode (Bioanalytical Systems, Inc.) coated with mercury. The measurements of the cobalt complexes were performed directly on the mercury drops produced by the CGME instrument (drop size ∼4.9 mg). The complex concentration was 1 ± 0.05 mM and the temperature 23 ± 1 °C in all experiments made to investigate the redox catalytic activity of the complexes toward CO_2.

The diffusion coefficient of the CO_2 molecule in ACN retrieved by the fitting routine was $\sim 3.5 \times 10^{-5}$ cm²/s. A similar value was also obtained from measuring the uncatalyzed reduction of CO_2 in DMF up to the saturation concentration at a gold disk electrode ($r = 0.8$ mm) coated with mercury, taking the viscosities of both solvents into account. The evaluation of the diffusion coefficient was performed by simulating working curves for the peak current on the basis of a totally irreversible charge-transfer process using the α values calculated from the $|E_p - E_{p/2}|$ potential difference. The calculations were done as two-dimensional simulations for a "real" disk electrode on account of non-negligible small part of spherical diffusion for $r = 0.8$ mm and low scan rates between 0.1 and 1 V/s.

2. Preparative-Scale Electrolyses. Preparativescale experiments were performed with the Wenking LB 95L potentiostat (Bank Electronics) in a gastight electrolysis cell under potentiostatic conditions. The applied potential was only ∼100 mV more negative than the standard potential of the complex to ensure that the working potential was always more positive than the potentials where the uncatalyzed reduction proceeded under the same conditions. The best results were obtained with a one-compartment cell using an aluminum wire as counter electrode. Before starting the electrolysis, the solution of 1 mM of the complex in ACN was saturated with CO_2 by bubbling the gas trough the electrolyte for ∼30 min. The working electrode was a mercury pool of ∼9 cm². The cell was equipped with a septum cup and an exchangeable cuvette for either ESR or UV−visible spectrophotometric investigations. Optical spectra were recorded on a Varian Cary 1 spectrophotometer. ESR measurements of electrochemically generated nickel(I) complexes were performed at 77 K either in DMF or in ACN using the ESR 200 (ZWG, Berlin) or the ESP 300E (Bruker) spectrometer. In the latter case, the electrolyses were performed in a two-compartment cell with glass frits and salt bridges between the cathodic and anodic compartment.

Samples from the gas phase were taken through the septum with a gas syringe and analyzed on Chrompack CP 9000 gas chromatograph using a molecular sieve and a Pora Plot Q column. The instrument was equipped with a thermal conductivity detector with helium as the carrier gas. This instrumentation allows the detection of both CO and H_2. At the end of the electrolyses, the products were identified by HPLC. For this purpose, the ACN was removed under reduced pressure and the precipitate was extracted with chloroform−water mixture to remove the supporting electrolyte and the rest of the complexes. The water extract was then directly analyzed on a Knauer liquid chromatograph equipped with a UV detector operating at 208 nm. The column was a Luna 5-μm C18(2) eluted with 5% H_3PO_4. The peak areas were calibrated by applying the above procedure to authentic samples of formic and oxalic acids as well as to their lithium salts. Additionally, the products of long-time electrolyses were analyzed by titration with $KMnO_4$. Although all of the oxalate was presumably precipitated during the electrolyses in the form of aluminum oxalate, an excess of $NaClO_4$ was added to the electrolyte at the end of the electrolyses to ensure a quantitative precipitation of the oxalate. The precipitate was filtrated, washed with ACN, and finally precipitated and recrystallized in water as calcium oxalate. The latter was titrated with $KMnO_4$ in the classical way.

Acknowledgment. The authors thank the Deutsche Forschungsgemeinschaft and the Fonds der Chemischen Industrie for financial support.

JA001254N